Pure Appl. Chem., Vol. 85, No. 1, pp. 237–246, 2013.
http://dx.doi.org/10.1351/PAC-CON-12-02-08

Lanthanoids(III) and actinoids(III) in water: Diffusion coefficients and hydration enthalpies from polarizable molecular dynamics simulations*

Fausto Martelli[1], Sacha Abadie[1], Jean-Pierre Simonin[2], Rodolphe Vuilleumier[3], and Riccardo Spezia[1,‡]

[1]Laboratoire Analyse et Modélisation pour la Biologie et l'Environnement, UMR 8587 CNRS-CEA-UEVE, Université d'Evry Val d'Essonne, Evry, France; [2]Laboratoire PECSA (UMR CNRS 7195), Université P.M. Curie, Paris, France; [3]Ecole Normale Supérieure, Département de Chimie, Paris, France, and UPMC Université Paris 06, UMR 8640 CNRS-ENS-UPMC, Paris, France

Abstract: By using polarizable molecular dynamics (MD) simulations of lanthanoid(III) and actinoid(III) ions in water, we obtained ionic diffusion coefficients and hydration enthalpies for both series. These values are in good agreement with experiments. Simulations thus allow us to relate them to microscopic structure. In particular, across the series the diffusion coefficients decrease, reflecting the increase of ion–water interaction. Hydration enthalpies also show that interactions increase from light to heavy ions in agreement with experiment. The apparent contradictory result of the decrease of the diffusion coefficient with decreasing ionic radius is tentatively explained in terms of dielectric friction predominance on Stokes' diffusive regime.

Keywords: actinides; hydration; lanthanides; molecular dynamics; thermodynamics; water.

INTRODUCTION

In the last few years, various experimental and theoretical studies have been devoted to understanding the hydration properties of lanthanoids(III), Ln [1]. Experimentally, many recent studies used X-ray absorption spectroscopy (XAS) in both EXAFS (extended X-ray absorption fine structure) and XANES (X-ray absorption near edge structure) domain [2,3]. In particular, the systematic XAS studies of Persson, D'Angelo, and co-workers on the full Ln(III) series [4,5] recently provided an almost definitive picture of hydration structure: Ln–water distances decrease almost linearly across the series, and the coordination number (CN) also decreases from 9 in the case of light atoms to 8 in the case of heavier ones in a smooth way. This was a latest confirmation that the so-called "Gadolinium break" does not hold, as previously remarked by Helm and Merbach [1], and by Spedding and co-workers [6], who had suggested this picture at the beginning of their series of studies [7].

From a theoretical point of view, various force fields have been proposed by the community for the study of hydration by means of molecular dynamics (MD) in bulk water at finite temperature [8–12].

Pure Appl. Chem.* **85, 1–305 (2013). A collection of invited papers based on presentations at the 32nd International Conference on Solution Chemistry (ICSC-32), La Grande Motte, France, 28 August–2 September 2011.
‡Corresponding author

In particular, recent studies agree that including polarization in the force field is a key ingredient to correctly reproduce structural properties [13–16]. This increasing number of studies was stimulated by the improved experimental description of hydration mentioned above. Amongst recent Ln(III)–water interaction potentials, our group has developed a force field that is able to reproduce almost perfectly the EXAFS signals of D'Angelo and the aforementioned structural data [17].

Actinoids(III), An, were less investigated than Ln(III). Structural data were reported experimentally up to Cf(III) [18–22] by means of XAS. Cm(III) was probably the only trivalent cation studied in explicit solvents by molecular simulations [23,24] before last year when Galbis et al. reported Monte Carlo simulations of Cf(III) in water [22] and Spezia and co-workers reported hydration properties of the whole An(III) series [22]. In this latter work, a polarizable force field was developed for An(III) in water similar to the one developed for Ln(III). The results obtained were in good agreement with the few structural data available in the literature. We summarize in Fig. 1 the decrease of Ln–water and An–water distances and the corresponding CN change across the series as obtained from previous polarizable simulations [17,25].

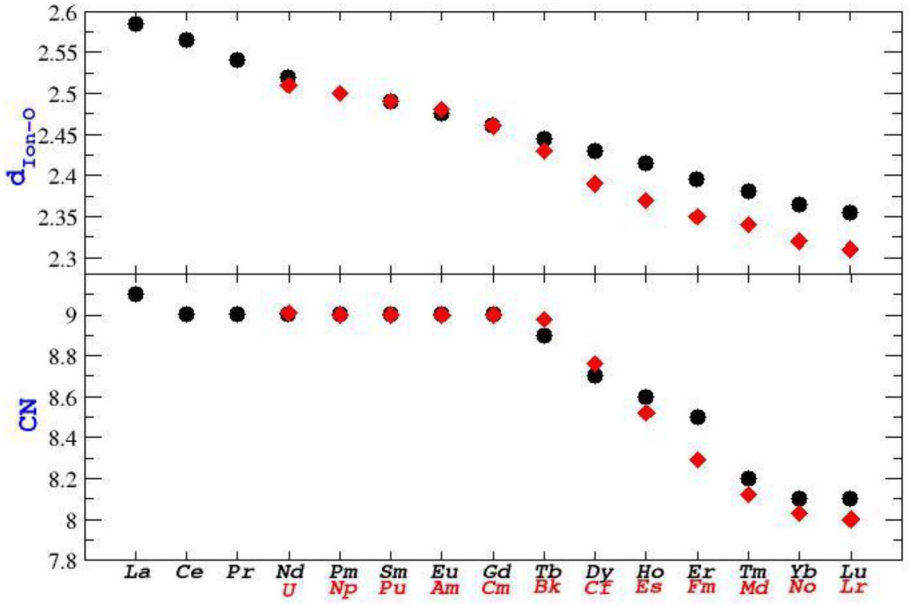

Fig. 1 First hydration shell CN in the Ln(III), circles, and An(III), diamonds, series as obtained from refs. [17,25], respectively.

The interest of understanding ion hydration in chemistry is, of course, not limited to structure. Thermodynamic properties like solvation energy and ionic diffusion coefficients are important quantities to characterize ionic solutions. Diffusion is related to the conductivity of solutions, for example, and solvation energy can be used to design liquid–liquid separation methods. For Ln(III) in water, experimental hydration energies were reported by Marcus [26], as well as for some An(III). Diffusion coefficients, *D*, were amongst the first properties reported experimentally. In fact, Spedding and co-workers measured in the 1950s the conductance of aqueous solutions of some rare earth at different concentrations [27–29] from which limiting values at infinite dilution were extrapolated for the solution conductivities and thus for the diffusion coefficients. Ln(III) diffusion coefficients were obtained later by Fourest et al. by using the open-ended capillary technique [30], confirming the previous data of

Spedding. At the same time, Fourest et al. also measured the diffusion coefficients of a few An(III) ions in water.

All these data agree in reporting a decrease of D across the series. Since D is related to the hydrodynamic radius by an inverse proportionality relationship according to Stokes' law, this means that the ionic radius should increase across the series. On the other hand, structural experiments reported a decrease of ion–water distance as well as of CN across the series that is in apparent contradiction with diffusion coefficient results. This can originate from a misinterpretation of XAS results, or from artifacts in the conductivity measurements. In particular, hydrolysis was excluded by Spedding and coworkers [28,29], and the agreement between conductance and the diffusion results of Fourest confirms that conclusion. Anyhow, the connection between these measurements and the microscopic hydration structure is still missing and unclear, so that some authors have defined some ad hoc radii that increase across the series, thus forcing them to follow Stokes' picture [30].

We have employed MD simulations with our recently developed force field in an attempt to bridge the gap between structural, thermodynamical, and mobility properties of Ln(III) and An(III) ions in water. Our model correctly reproduces the structures suggested by XAS and, as we can anticipate, also the diffusion coefficient behavior across the series. Coupling this data with hydration energies—for which we also found a good agreement with experiments—we will discuss the diffusion coefficients behavior in terms of hydration structure and ion–water interaction. In particular, the opposite behavior of the diffusion coefficient and ionic radius will then be discussed considering the dielectric friction [31]. The decrease of the diffusion coefficient across the series then follows the increase of interaction energy between the ion and the solvent.

METHODS

MD simulations of ion hydration were performed immersing one ion, Ln^{3+} or An^{3+}, in a box containing explicit water molecules, where periodic boundary conditions (PBCs) were applied in order to mimic bulk systems. Three cubic box sizes were employed: (i) a small box containing 216 water molecules with an edge of 18.68 Å; (ii) a medium box, containing 500 water molecules with an edge of 24.84 Å; (iii) a large box, containing 1000 water molecules with an edge of 31.05 Å. Ewald summations were employed for long-range interactions [32]. Simulations were done at room temperature, generating velocities at 300 K followed by an equilibration MD run at the target temperature. Then NVE simulations were performed for 3 ns. We have checked that room temperature was maintained throughout the simulations.

Ion–water and water–water interactions were treated using a pair potential in which polarization effects were included in the electrostatic term by means of Thole's induced dipole model [33]. Atomic dipoles were calculated at the beginning by using a self-consistent procedure and then propagated by adding an associated dynamical variable and fictitious mass to the system Hamiltonian as proposed by Sprik a few years ago [34]. Water molecules were modeled via a modified rigid TIP3P model [35] that accounts for polarizability on atomic sites [36] while ion–water non-electrostatic interactions were modeled using a Buckingham pair potential of the form

$$V = Ae^{-Br} - \frac{C}{r^6} \tag{1}$$

where r is the ion–oxygen distance and A, B, C are Ln–water and An–water parameters obtained in our group's previous work. They reflect the decrease of ionic radii across the series [17,25]. More details on the simulation methods can be found in our previous works on structural properties [15]. All simulations were performed using the MDVRY code [37].

The diffusion coefficient values were calculated from simulations via the well-known relationship

$$D_{\mathrm{PBC}} = \lim_{t\to\infty} \frac{\partial}{\partial t} \frac{\left\langle \left|\mathbf{r}(t) - \mathbf{r}(0)\right|^2 \right\rangle}{6} \tag{2}$$

where D_{PBC} is the value obtained for each simulation box. Since, as shown by Hummer and co-workers [38], they depend on simulation box size when PBCs are employed, we extrapolate the infinite box values that correspond to infinite dilution from the values obtained for each ion at a different box dimension. In the results section below, we only report the extrapolated values.

Finally, from simulations we calculated the hydration enthalpies by subtracting the internal energy of pure solvent from the internal energies for the systems composed of ions and water. This, as described in detail by Garcia, McCammon, Hunenberger and co-workers [39–41], requires a series of corrections to recover the correct thermodynamic quantities and avoid errors due to the use of PBC. Corrections were evaluated and applied. In the results section, we report results for the large simulation boxes where, as expected, corrections are also smaller.

RESULTS

From simulations of Ln(III) ions in water, we obtained ionic limiting diffusion coefficients (see Table 1). In the same table, we show experimental values reported by Spedding [29] and Fourest [30] from conductivity and diffusion measurements, respectively. The values reported by Spedding and coworkers were obtained at different concentrations, from which one can get the diffusion coefficients from the well-known relation [42]

$$D = \frac{RT\lambda}{F|z|} \tag{3}$$

where λ is the measured conductance, T is the temperature, R is the gas constant, F is the Faraday constant, and z is the valence of the ion. In Table 1 we report values obtained assuming $z = +3$, which corresponds to the absence of hydrolysis, as supposed by the original authors. A first validation of this hypothesis comes from the agreement with values reported by Fourest et al. that were obtained from mobility measurements. A further confirmation is brought by comparison with simulations, where by definition no hydrolysis occurs since we use a classical water model in which chemical bonds are not allowed to break. It should be noticed that in all density functional theory (DFT)-based simulations of a Ln(III) ion in water reported in the literature spontaneous hydrolysis was never observed [43–45].

As shown in Table 1, simulated and experimental values agree well. While there is some deviation—of small magnitude—between simulations and experiments, our simulations reproduce the decrease of the diffusion coefficients across the series. The study of Floris and Tani reported Ln(III) in water diffusion coefficients from simulations [9]. They found a relatively large discrepancy with respect to experiments, and, more importantly, not the expected decrease across the series. The latter result is probably due to the fact that they did not find the correct decrease in CN, as we conversely do. Note that our simulations show that it is physically possible that, to a decrease of Ln–water distance, or ionic radii, and CNs across the series, also corresponds a decrease of diffusion coefficients. We will discuss in more detail the physical basis of this observation below. Finally, the good agreement confirms the hypothesis that the experiments were not contaminated by hydrolysis, or at least only to a small extent.

Table 1 Diffusion coefficients for Ln(III) in water. We also show literature values from both experiments and simulations.

	$D \times 10^6$ ($cm^2\ s^{-1}$) this work[a]	$D \times 10^6$ ($cm^2\ s^{-1}$) simulations[b]	$D \times 10^6$ ($cm^2\ s^{-1}$) experiments[c]	$D \times 10^6$ ($cm^2\ s^{-1}$) experiments[d]
La^{3+}	6.29			6.16–6.18
Ce^{3+}	6.26		6.20(5)	6.16–6.19
Pr^{3+}	6.12			6.15–6.17
Nd^{3+}	6.18	3.5		6.15–6.19
Sm^{3+}	6.09			6.07–6.09
Eu^{3+}	5.85		6.02(4)	6.01
Gd^{3+}	5.76	3.5	5.74(5)	5.95–5.99
Tb^{3+}	5.64		5.79(5)	5.92–5.93
Dy^{3+}	5.57			5.88
Ho^{3+}	5.65			5.87–5.89
Er^{3+}	5.61			5.81–5.85
Tm^{3+}	5.71		5.80(5)	5.80
Yb^{3+}	5.39	4.4	5.78(5)	5.77–5.85
Lu^{3+}	5.52			5.73

[a]From simulations we can estimate an uncertainty of 0.2×10^{-6} $cm^2\ s^{-1}$.
[b]Simulations of Floris and Tani from ref. [9].
[c]From open-ended capillary technique of Fourest et al. [30]. Uncertainties are reported in parenthesis.
[d]From limiting ionic conductance measurements of Spedding et al. [29] with various counterions (Cl^-, Br^-, ClO_4^-, NO_3^-, SO_4^{2-}) by using eq. 3. Uncertainties were not reported by the authors.

As already discussed, we have recently developed a force field for An(III) series in water [25]. While for Ln(III) we were able to directly couple simulations with experiments, so providing effective ionic radii and a set of parameters that provides a perfect agreement with XAS experiments, this was not possible for An(III), due to the lack of experiments on the whole series (and the access for us to the spectra of studied species). In our force field developing work, we have thus reported different sets of parameters corresponding to different ionic radii: r_9 corresponding to a crystal structure coordination number (CSCN) of 9, r_8 for CSCN = 8, and $r_{8.5}$ for the intermediate case, as detailed in ref. [25]. In Table 2, we report diffusion coefficient values obtained from each set of parameters and compare them with available experimental data.

Table 2 Diffusion coefficients for An(III) in water[a].

	$D \times 10^6$ (cm^2 s^{-1}) r_9	$D \times 10^6$ (cm^2 s^{-1}) $r_{8.5}$	$D \times 10^6$ (cm^2 s^{-1}) r_8	$D \times 10^6$ (cm^2 s^{-1}) simulations[b]	$D \times 10^6$ (cm^2 s^{-1}) Experiments[c]
U^{3+}	6.17				
Np^{3+}	6.14				
Pu^{3+}	6.16				
Am^{3+}	6.26				6.25(3)
Cm^{3+}	5.87			5.2	6.12(6)
Bk^{3+}	5.88	5.90	5.98		
Cf^{3+}	5.92	5.82	5.87		5.87(4)
Es^{3+}	5.63	5.64	5.67		5.77(5)
Fm^{3+}	5.67	5.81	5.78		
Md^{3+}	5.23	5.62	5.74		
No^{3+}	5.24	5.45	5.32		
Lr^{3+}	5.33	5.43	5.25		

[a]Uncertainties of our simulations are evaluated to be 0.2×10^{-6} cm^2 s^{-1}.
[b]From simulations of Atta-Fynn et al. [46].
[c]From open-ended capillary method of Fourest et al. from ref. [30]. Uncertainties are reported in parenthesis.

Results are in good agreement with available experiments, and we can use this comparison to choose the best set of parameters, especially for atoms where XAS structural data are not available. From U^{3+} to Cm^{3+}, r_9 seems to be preferable: some discrepancies in D are counterbalanced by a very good agreement with the available XAS experiments [19]. For Bk^{3+} and Cf^{3+}, $r_{8.5}$ is the preferred set following comparison with XAS data [20–22], albeit in the case of Cf^{3+}, r_8 diffusion coefficients agree better (within the uncertainty of both experiments and simulations). Finally, for the heavier cations, from Es^{3+} to Lr^{3+}, r_8 is the preferred set. In this case, we can compare only D of Es^{3+}, since XAS data are not available for any of them. We thus keep r_8 parameters also up to the end of the series. This is due to the fact that ionic radii are a function of CN and we can estimate that they decrease linearly from Es^{3+} to Lr^{3+} for the following reason: An–O distances, which reflect ionic radii, obtained by quantum chemistry calculation in the presence of implicit solvent are almost linear [47]. Thus, using r_9 or $r_{8.5}$ set after Es^{3+}, for which r_8 provided the best agreement, will break this coherent decreasing behavior. This is of course a hypothesis, but up to now we do not have any other experimental data to compare with for the heavier cations.

Finally, we obtained from simulations the hydration enthalpy (ΔH_{hydr}). We compared these values with the experimental ones reported by Marcus [26] for the whole Ln^{3+} series and for two An^{3+} ions (U^{3+} and Pu^{3+}). In Table 3 we report ΔH_{hydr} obtained by simulations and experiments. We found globally a good agreement with differences not larger than 85 kJ/mol, and a mean unsigned error of 44 kJ/mol (which is less than 2 % of the energy values). Note that this is typical of observed differences when comparing simulated and experimental hydration energies, for which experimental uncertainties are also of the same order of magnitude. Kowall et al. [8] reported hydration enthalpies for Nd^{3+}, Sm^{3+}, and Yb^{3+}, and Villa et al. [48] for Nd^{3+}, Gd^{3+}, and Yb^{3+}, both finding a similar or bigger difference with respect to the same Marcus data. We observe a global decrease of hydration enthalpy that corresponds to a strengthening of water–ion interaction across the series. A little increase at the end of the series (observed experimentally) is also found in our simulations.

Table 3 Ln(III) and An(III) hydration enthalpies, ΔH_{hydr}, in kJ/mol.

	Simulations[a]	Experiments[b]
La^{3+}	–3395	–3310
Ce^{3+}	–3382	–3365
Pr^{3+}	–3441	–3410
Nd^{3+}	–3429	–3445
Sm^{3+}	–3561	–3490
Eu^{3+}	–3612	–3535
Gd^{3+}	–3617	–3545
Tb^{3+}	–3621	–3580
Dy^{3+}	–3614	–3600
Ho^{3+}	–3674	–3635
Er^{3+}	–3740	–3670
Tm^{3+}	–3762	–3695
Yb^{3+}	–3721	–3740
Lu^{3+}	–3751	–3695
U^{3+}	–3445	–3435
Np^{3+}	–3527	
Pu^{3+}	–3511	–3525
Am^{3+}	–3634	
Cm^{3+}	–3552	
Bk^{3+}	–3451	
Cf^{3+}	–3664	
Es^{3+}	–3625	
Fm^{3+}	–3688	
Md^{3+}	–3664	
No^{3+}	–3749	
Lr^{3+}	–3798	

[a]Uncertainties in simulations are of 11 kJ mol^{-1}.
[b]Experimental values from Marcus [26].

ΔH_{hydr} correlates well with ion–water distances and CNs, as already remarked by Fujiwara et al. [49] for a few Ln^{3+}. The increase of water–cation interaction across the series correlates well also with the observed decrease of diffusion coefficients, as shown in Fig. 2. Across the series, as the ion–water interaction increases, the ion diffuses more slowly.

But this behavior is reversed to what can be espected from Stokes' law based ionic radii. When Stokes' law does not fit with the ionic radius, one usually evokes a "hydrodynamic" radius that is greater than the ionic radius. This was done by Fourest et al. [30] in order to explain the decrease of diffusion coefficients in Ln(III) and An(III) series, from which they evaluated ionic radii increase from 4.53 to 4.67 Å and from 4.51 to 4.68 Å, respectively, for each series. These radii are much larger than the first neighbors distances. If we look, however, at the second hydration shell of the two series as obtained by simulations [15,25], we still find also a (small) decrease of the ion–water distance, still in contradiction with the decrease of the diffusion coefficients. Alternatively, similarly to Li^+, one may suggest that the first-solvation shell motion is more correlated to the ion motion. However, the residence times of water molecules in the first solvation shell are very long for all ions in the lanthanide and actinide series, larger than few hundreds picoseconds and up to nanoseconds, and their variation along the series is non-monotonic, the residence times being shortest in the middle of the series [10]. Thus, it seems impossible to associate the decreasing diffusion constant with the behavior of any structural distance across the series.

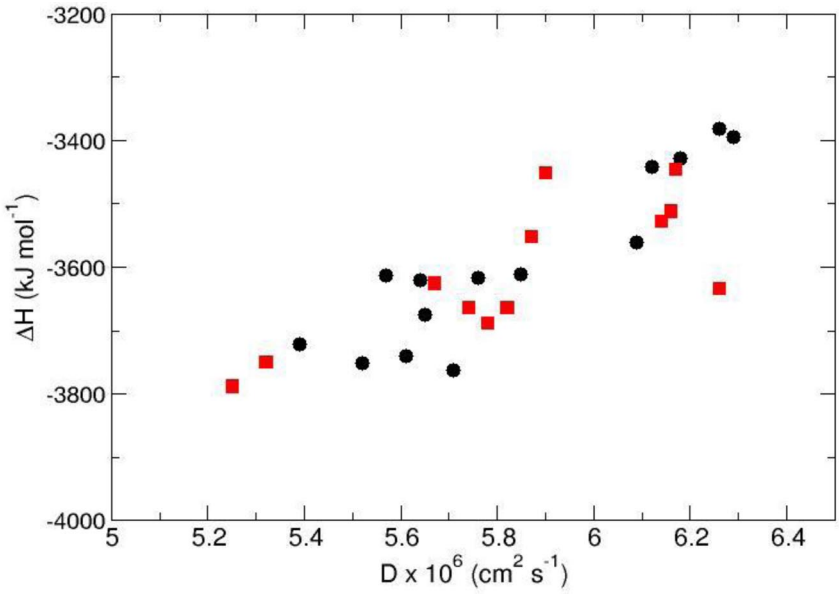

Fig. 2 Hydration enthalpy as a function of diffusion coefficient for Ln(III), in circles, and An(III), in squares, series obtained from MD simulations in water.

A quantitative description of the observed phenomenon can be obtained from the Hubbard–Onsager theory of solvated ion dynamics [31]. Following Hubbard–Onsager theory, one can express the ionic friction coefficient in solution as

$$\zeta = 4\pi\eta R + \left(\frac{1}{15}\right)\frac{\tau_D e^2}{R^3}\left(\frac{\varepsilon_0 - \varepsilon_\infty}{\varepsilon_0^2}\right) \tag{4}$$

where $\zeta = kT/D$, η is the pure solvent viscosity, R the solute radius (the ionic radius for ions in solution), τ_D the solvent dielectric relaxation time, e the solute charge, and ε_0 and ε_∞ the static and high-frequency dielectric constants of pure solvent, respectively. The first term of the right-hand side of eq. 4 is the well-known viscous friction contribution corresponding to Stokes' law for slip diffusion. According to the first term only, the diffusion coefficient should increase as the ionic radius decreases. The second term is what Hubbard and Onsager (and also Zwanzig [50] and Adelman [51]) defined as originating from dielectric friction. This term has an opposite behavior than the Stoke's contribution as a function of ionic radius, which is in agreement with what is observed for Ln(III) and An(III) ions in water. We can evaluate the two terms and see that, in the case of trivalent ions, assuming R to be in the range 1.250–0.995 Å (the effective ionic radii of Ln^{3+} in water [17]), the second term is predominant. This can provide a qualitative explanation of the observed trend in the diffusion coefficients. Note that the Hubbard–Onsager picture provides diffusion coefficients that have the same order of magnitude as observed, i.e., in the range 4.79×10^{-6} to 2.68×10^{-6} cm^2 s^{-1}. This semiquantitative justification explains why ions with decreasing ionic radii show also decreasing diffusion coefficients. The correlation of the diffusion coefficient with the hydration energy is then the expression of the stronger coupling of the ion with the polarization field of the solvent along the series.

CONCLUSIONS

In this paper, we have found that our polarizable potential for simulating Ln(III) and An(III) in liquid water, developed in order to accurately reproduce structural properties, is also able to reproduce exper-

imental diffusion coefficients and hydration enthalpies. This brings support to the conclusion that the polarizability is a key ingredient to make the ion–water potential transferable. Surely, thermodynamics is related to interaction potential and for highly charged cations, like Ln(III) and An(III), the electrostatic contribution is predominant in determining not only the hydration enthalpy but also the diffusion properties. Indeed, estimating the two terms in the Hubbard–Onsager theory that takes into account also the dielectric friction, it is shown that the former has predominance over the Stokes' term for such small and highly charged ions. Surely, this is still a crude model and a better description, similar to the Adelman model [51], will be necessary to have a deeper understanding on the physical-chemical properties of hydration and mobility of small ions. Our simulations show that the contradiction between the experimental decrease of diffusion coefficients along the Ln(III) and An(III) series, together with a decrease of ion–water distances (and ionic radii) and CN across the same two series, is only apparent and can be related to dielectric friction, without relying on another hypothesis like hydrolysis of first-shell waters.

ACKNOWLEDGMENTS

This research was supported by the ANR 2010 JCJC 080701 ACLASOLV (Actinoids and Lanthanoids Solvation) and GNR PARIS 2010.

REFERENCES

1. L. Helm, A. E. Merbach. *Chem. Rev.* **105**, 1923 (2005).
2. J. Näslund, P. Lindqvist-Reis, I. Persson, M. Sandström. *Inorg. Chem.* **39**, 4006 (2000).
3. P. D'Angelo, A. Zitolo, V. Migliorati, I. Persson. *Chem.—Eur. J.* **16**, 684 (2010).
4. I. Persson, P. D'Angelo, S. De Panfilis, M. Sandstrom, L. Eriksson. *Chem.—Eur. J.* **14**, 3056 (2008).
5. P. D'Angelo, S. De Panfilis, A. Filipponi, I. Persson. *Chem.—Eur. J.* **14**, 3045 (2008).
6. F. H. Spedding, M. J. Pikal, B. O. Ayers. *J. Phys. Chem.* **70**, 2440 (1966).
7. (a) A. Habenschuss, F. H. Spedding. *J. Chem. Phys.* **70**, 3758 (1979); (b) A. Habenschuss, F. H. Spedding. *J. Chem. Phys.* **70**, 2797 (1979); (c) A. Habenschuss, F. H. Spedding. *J. Chem. Phys.* **73**, 442 (1980).
8. T. Kowall, F. Foglia, L. Helm, A. E. Merbach. *J. Am. Chem. Soc.* **117**, 3790 (1995).
9. F. M. Floris, A. Tani. *J. Chem. Phys.* **115**, 4750 (2001).
10. M. Duvail, R. Spezia, P. Vitorge. *ChemPhysChem* **9**, 693 (2008).
11. C. Clavaguéra, R. Pollet, J. M. Soudan, V. Brenner, J. P. Dognon. *J. Phys. Chem. B* **109**, 7614 (2005).
12. C. Beuchat, D. Hagberg, R. Spezia, L. Gagliardi. *J. Phys. Chem. B* **114**, 15590 (2010).
13. A. Villa, B. Hess, H. Saint-Martin. *J. Phys. Chem. B* **113**, 7270 (2009).
14. M. Duvail, M. Souaille, R. Spezia, T. Cartailler, P. Vitorge. *J. Chem. Phys.* **127**, 034503 (2007).
15. M. Duvail, P. Vitorge, R. Spezia. *J. Chem. Phys.* **130**, 104501 (2009).
16. F. Lipparini, V. Barone. *J. Chem. Theory Comput.* **7**, 3711 (2011).
17. P. D'Angelo, A. Zitolo, V. Migliorati, G. Chillemi, M. Duvail, P. Vitorge, S. Abadie, R. Spezia. *Inorg. Chem.* **50**, 4572 (2011).
18. B. Brendebach, N. L. Banik, Ch. M. Marquardt, J. Rothe, M. A. Denecke, H. Geckeis. *Radiochim. Acta* **97**, 701 (2009).
19. S. Skanthakumar, M. R. Antonio, R. E. Wilson, L. Soderholm. *Inorg. Chem.* **46**, 3285 (2007).
20. R. Revel, C. Den Auwer, C. Madic, F. David, B. Fourest, S. Huber, J. F. Le Du, L. R. Morss. *Inorg. Chem.* **38**, 4139 (1999).
21. M. R. Antonio, L. Soderholm, C. W. Williams, J.-P. Blaudeau, B. E. Bursten. *Radiochim. Acta* **89**, 17 (2001).

22. E. Galbis, J. Hernandez-Cobos, C. Den Auwer, C. Le Naour, D. Guillaumont, E. Simoni, R. R. Pappalardo, E. Sanchez-Marcos. *Angew. Chem., Int. Ed.* **49**, 3811 (2010).
23. T. Yang, B. E. Bursten. *Inorg. Chem*. **45**, 5291 (2006).
24. D. Hagberg, E. Bednarz, N. M. Edelstein, L. Gagliardi. *J. Am. Chem. Soc.* **129**, 14136 (2007).
25. M. Duvail, F. Martelli, P. Vitorge, R. Spezia. *J. Chem. Phys.* **135**, 044503 (2011).
26. Y. Marcus. *Biophys. Chem.* **51**, 111 (1994).
27. F. H. Spedding, P. E. Porter, J. M. Wright. *J. Am. Chem. Soc*. **74**, 2055 (1952).
28. F. H. Spedding, J. L. Dye. *J. Am. Chem. Soc*. **76**, 879 (1954).
29. F. H. Spedding, R. A. Nelson, J. A. Rard. *J. Chem. Eng. Data* **19**, 379 (1974).
30. B. Fourest, J. Duplessis, F. David. *Radiochim. Acta* **36**, 191 (1984).
31. J. Hubbard, L. Onsager. *J. Chem. Phys.* **67**, 4850 (1977).
32. U. Essmann, L. Perera, M. L. Berkowitz, T. Darden, H. Lee, L. G. Pedersen. *J. Chem. Phys.* **103**, 8577 (1995).
33. B. T. Thole. *Chem. Phys.* **59**, 341 (1981).
34. M. Sprik. *J. Phys. Chem.* **95**, 2283 (1991).
35. W. L. Jorgensen, J. Chandrasekhar, J. D. Madura, R. W. Impey, M. L. Klein. *J. Chem. Phys.* **79**, 926 (1983).
36. P. van Duijnen, M. Swart. *J. Phys. Chem. A* **102**, 2399 (1998).
37. M. Souaille, H. Loirat, D. Borgis, M.-P. Gaigeot. *Comp. Phys. Commun*. **180**, 276 (2009).
38. I.-C. Yeh, G. Hummer. *J. Phys. Chem. B* **108**, 15873 (2004).
39. G. Hummer, L. R. Pratt, A. E. Garcia. *J. Phys. Chem.* **100**, 1206 (1996).
40. P. H. Hunenberger, J. A. McCammon. *J. Chem. Phys.* **110**, 1856 (1999).
41. (a) M. A. Kastenholz, P. H. Hunenberger. *J. Chem. Phys.* **124**, 124106 (2006); (b) M. A. Kastenholz, P. H. Hunenberger. *J. Chem. Phys.* **124**, 224501 (2006).
42. R. A. Robinson, R. H. Stokes. *Electrolyte Solutions*, 2nd ed., Butterworths, London (1959).
43. C. Terrier, P. Vitorge, M.-P. Gaigeot, R. Spezia, R. Vuilleumier. *J. Chem. Phys.* **133**, 044509 (2010).
44. T. Ikeda, M. Hirata, T. Kimura. *J. Chem. Phys.* **122**, 244507 (2005).
45. O. V. Yazyev, L. Helm. *J. Chem. Phys*. **127**, 084507 (2007).
46. R. Atta-Fynn, E. J. Bylaska, G. K. Schenter, W. A. de Jong. *J. Phys. Chem. A* **115**, 4665 (2011).
47. J. Wiebke, A. Moritz, X. Cao, M. Dolg. *Phys. Chem. Chem. Phys*. **9**, 459 (2007).
48. A. Villa, B. Hess, H. Saint-Martin. *J. Phys. Chem. B* **113**, 7270 (2009).
49. T. Fujiwara, H. Mori, Y. Mochizuki, E. Miyoshi. *J. Mol. Struct. THEOCHEM* **949**, 28 (2010).
50. R. Zwanzig. *J. Chem. Phys.* **52**, 3625 (1970).
51. J.-H. Chen, S. A. Adelman. *J. Chem. Phys*. **72**, 2819 (1980).

